Term Paper

Using Cross-Correlated, Head-Wave and Diving-Wave Seismic Energy To Position Ocean Bottom Seismic Cables

Noel Zinn
University of Houston
GEOL 7333: Seismic Wave and Ray Theory
Professor Robert E. Sheriff
Spring 1999

Date Due: April 8, 1999

Date Submitted: April 6, 1999

www.hydrometronics.com

Using Cross-Correlated, Head-Wave and Diving-Wave Seismic Energy To Position Ocean Bottom Seismic Cables

Noel Zinn
University of Houston
GEOL 7333: Seismic Wave and Ray Theory
Spring 1999

Preface

In a lecture to Dr. Sheriff's Reservoirs class this semester, Jack Caldwell of Schlumberger GECO-Prakla discussed several seismic ocean-bottom cable (OBC) issues. I will focus on one of those issues, OBC detector positioning, for which Caldwell offers acoustics as the only solution. However, seismic energy itself (first breaks) can also be used to position OBC detectors. Furthermore, seismic energy does not suffer the depth limitations of the current generation of OBC acoustics, a concern raised by Caldwell for deeper-water OBC surveys of the future.

In this paper I offer an overview of OBC and OBC positioning methods, including seismic first breaks. Next, I offer a brief description of the 1997 Texaco Teal South OBC survey from which I have extracted real seismic traces for first-break picking and normalized cross correlations in Matlab later in the paper. Next, I present a geological model in Matlab that traces head waves using the ray parameter to simulate first breaks for the testing of the generic positioning algorithm presented later. Next, I turn my attention to the first break picking of seismic traces from Teal South using different techniques including normalized cross correlation. Next, I describe a generic processing algorithm that models vertical velocity gradients with a polynomial and converts the first-break time picks of head waves and diving waves into distances that are processed by least squares to estimate detector positions. Finally, I exhibit the sub-meter comparisons between first-break and acoustic coordinates for the Teal South survey.

Marine seismic positioning is my profession. Although this paper does draw on some material I've written previously (see references), it mostly includes new material covered in this Seismic Wave and Ray Theory class. The reprise of head-wave and diving-wave propagation, ray tracing through the sedimentary layers, the principle of least squares and the processing method of cross correlation to determine static corrections (or first breaks in this case) are all topics covered in class or in the assigned reading. These topics are increasingly important to me professionally. Although we haven't covered it in class, some of our text is devoted to the positioning of land and marine seismic surveys, an issue often neglected by uninformed geophysicists, an issue that can affect the quality of our seismic interpretation. So, this paper blends what I know with what I've set out to learn by taking this and other classes at the University of Houston. This paper also addresses a specific deficiency (albeit minor) of the Caldwell lecture.

Acknowledgements are mentioned at the end of the paper.

Overview of Ocean Bottom Cable Seismic Surveying

Reflection seismology is the primary geophysical method employed in the search for hydrocarbon accumulations. Seismic data are collected on land, at sea and in the transition zones in between land and sea. On land, seismic geophone sensors embedded in the earth and energy sources under the earth or at the surface are positioned conventionally (i.e., with theodolites and EDMI) or with the Global Positioning System (GPS). At sea, often called deep-marine seismic, seismic energy

sources (typically air guns) and seismic hydrophone sensors towed behind a vessel are positioned by a variety of devices that include GPS, magnetic compasses, underwater acoustics, lasers and optical shaft encoders. The data from these sensors are integrated into a total network algorithm processed by least squares or a least-squares-derivative Kalman filter (Zinn and Rapatz, 1993). In the transition zone of shallow surf, mud and alligators, we use any combination of these technologies that gets the job done.

In the marine environment, ocean bottom cable (OBC) surveying, in which the seismic cable is laid on the bottom, not towed near the surface, is gaining popularity. Some of the advantages of OBC over towed streamer surveys are a flexibility of acquisition geometry that resembles land more than marine, greater surface consistency (i.e., more combinations of source and detector at different azimuths and offsets for a given midpoint, useful for resolving static delays and for amplitude compensation, cf. Sheriff and Geldart, pages 303-305), more flexibility in working around obstructed zones, the use of dual sensors (pressure hydrophones and acceleration geophones, which are 90 degrees out of phase, cf. Sheriff and Geldart, page 293) to remove ghosts and layer reverberations, multi-component geophones on the ocean bottom to record shear waves, reduced noise by eliminating cable vibration and strumming caused by towing and surface weather conditions, and better coverage due to the elimination of cable feather caused by currents.

Figure 1 shows the important elements of an OBC survey. There are cables with dual seismic sensors (hydrophones and geophones) connected to a recording vessel in the middle of the graphic. The shooting vessel with one or more air gun arrays that produce the seismic energy is shown sailing a regular pattern orthogonally to the cables. Orthogonal shooting has geophysical and geodetic (positioning) advantages, but in-line shooting is also possible. The collected midpoints of all possible combinations of sources and detectors comprise a swath of coverage.

OBC surveys are today limited to about 200 meters of water depth, but 1000-meter surveys may be commonplace in a couple of years. The refracted-energy, first-break techniques described in this paper are as applicable to 1000-meter depths as to 10-meter depths.

Positioning Methods

Seismic energy source positioning in OBC is similar in technique and quality to source positioning in deep-water streamer surveys. It basically consists of GPS antennas on the source array. On the other hand, detector positioning techniques are less-widely standardized in OBC than in land or towed-streamer surveys. Three techniques are common in the industry: (1) recording and using the drop or placement coordinates of the detectors, (2) deploying high-frequency acoustic sensors attached to the detectors and positioned independently of the seismic survey and (3) using multiple occasions of the onset of seismic energy (first breaks) as surveying observations in a positioning algorithm, a viable alternative to acoustics not mentioned by Caldwell. A combination of acoustics and first breaks is also possible.

Drop Coordinates

Since drop positions must be recorded to assure that the actual detector locations are near the planned locations, drop positions are the cheapest and easiest to implement. In calm shallow water (such as an inland bay where the detectors may be placed on or thrust into the muddy bottom), the detector drop position can be close to the resting position. In deeper water or in agitated surf zones, this is unlikely due to waves, currents and drop trajectories.

Acoustics

High-frequency (60 kHz) acoustic systems, which are technologically similar to those used for years in deep-marine surveys, are available for OBC applications. An acoustic transducer on a survey vessel interrogates transponders attached near the seismic detectors to determine their positions. Transducer positions and acoustic responses are processed in an adjustment algorithm (Cross 1983, Gelb 1974) to derive transponder positions.

Acoustics provide a precise observable (see next paragraph), essentially a time pick computed in hardware. Consequently, acoustic surveys can be quite accurate within their budget of systematic errors that includes uncertainties in detector depth, the velocity of sound in water and instrumental delay between the acoustic interrogation and the transducer's GPS coordinates. Acoustic processing software must account for vessel motion and successfully reject outlying responses caused by surface ghosts or vessel noise. Acoustics can save time by providing rapid positions when they are needed, but this is accomplished at the expense of dedicated equipment and personnel.

One acoustic vendor reports a measurement resolution of 100µs; another reports 13µs. Independent static tests confirm a precision of 60 to 80µs for both systems. This static precision is the equivalent to about 10cm in terms of distance in water. In production least-squares adjustments during seismic surveys, acoustic residuals more typically average 0.6 to 1.0m than 0.10m. This larger figure includes the effects of environmental and systematic sources of error. Normal (in-line) acoustic "pinging" geometry decreases the resistance of acoustics to positional shifts due to unrejected outliers. Acoustics are not reliable if executed poorly. ("Reliability" has a technical meaning in geodesy described by Zinn, January 1998).

First Breaks

Seismic first-breaks can be picked by any number of automated methods that choose a significant change in the amplitude or inflection of the arriving seismic energy. Figures 6, 7 and 8 show some seismic traces. A trace can be preconditioned by band-pass filtering or by deconvolution to improve signal-to-noise ratio and wavelet resolution. Automated picking can be enhanced with neural networks, or especially troublesome picks can be made by hand. Resolution can also be increased by interpolation between the samples with a sinc function. First-break picking by the methods of amplitude change and cross correlation is discussed in Section 6.

The time of a first-break pick can be related to distance. Distances can be processed in a positioning algorithm. A generic positioning algorithm is described in Section 7.

First-break positioning potentially combines the cost advantages of drop positions with the accuracy of acoustics. In an OBC survey, the marginal cost of picking and processing first breaks is low since the personnel, software, and seismic data are already on the job. Although each first break is a crude observable by navigation standards, we enjoy an abundance of observations, especially when refracted, head-wave energy is processed. Head wave energy is ray traced in Section 5. Pick quality is discussed in Section 6.4.

Laws of statistical error cancellation in a large sample of random observations readily confirm that acoustic-quality results are possible with first breaks. First-break positioning software must correctly compensate for detector depth, the velocity of propagation through water and one or more refractors, instrumental delay, picking delay (or anticipation) and, possibly, a complex near-surface geology. It must successfully reject outlying picks caused by noisy seismic data. The surface consistency of 3D OBC (i.e., the great variety of offset and azimuth as a consequence of shooting lines perpendicular to the detector lines) enhances the reliability of the first-break coordinate solution (cf. Zinn, January 1998).

Combination of Acoustics and First Breaks

Acoustics and first breaks are very different positioning technologies. A combination of these methods provides positioning redundancy and independent assurance that coordinates are adequate for seismic purposes. Acoustics provide highly precise observations, but usually fewer of them. First breaks provide a relative abundance of observations, albeit of lesser quality. A bullet-plot comparison of acoustic and first-break positions is given in Section 8.

Texaco Teal South Prospect

The real data examined in this paper were taken from the Texaco Teal South field, which is located in the Eugene Island area of the Gulf of Mexico. The field is a shallow reservoir with prolific production rates since coming on line in the mid 1990s, but with a short projected life. Texaco identified a need for a 4-D/4-C survey over the field to aid in the reservoir characterization, allowing improved production management to maximize the life of the field. An *in-situ* OBC survey was chosen since the water depths (75 to 85 meters) allowed easy deployment of the cables without the need for a costly remotely-operated vehicle (ROV). The survey size was small enough, requiring only 24 detector locations, so that significant capital resources would not be tied up by leaving the receiver cables in place (Ebrom et al 1998).

The first phase of the time-lapse survey was shot in 1997. Four 1000-meter detector cables, each with six multi-component phones 200 meters apart, were spaced in parallel, 400 meters north and south of one another. They were laid under tension both to aid receiver group spacing and alignment of the in-line horizontal geophones. A nine square kilometer grid of shots spaced 25m by 25m (14,397 shots) was acquired into the 24 deployed detector locations, providing a 24-fold survey into 12.5m square bins. Figure 2 is an overview of all detectors and shots in the Teal South survey. The shot gaps to the west of the detector lines were caused by avoiding floating recording buoys. The shot gaps to the east of the prospect were caused by avoiding a platform and its tenders.

First-break positioning analysis was performed on the data set for final positioning. Verification of proper spacing of the detector line locations was accomplished in the field using an acoustic positioning system. This provided a unique opportunity to compare the results of both these positioning systems as well as to ensure that positioning of the survey was of the highest standard. Coordinate differences from the first phase of the Teal South survey are reported in Section 8.

The Propagation of Diving Waves and Head Waves

The Many Paths

Although Figure 3 is a cartoon, it illustrates many of the paths seismic energy may take to travel from an OBC source to the detectors laid on the ocean bottom. On the left is a source vessel towing a submerged air gun source. Spread out from left to right are detectors laid along the ocean bottom. The cable connecting the detectors is not seen. Notice that the detectors may lie on different bottom materials, possibly with different velocity characteristics, thus creating statics problems. Direct water paths of the seismic energy are shown to the left of the cartoon. Detectors near the source will receive their first arrival through the water. A secondary water arrival may be a ghost reflection from the surface, as shown. Detectors farther from the source will receive their first arrival through the earth under the ocean bottom. The cartoon shows a particular ray path with several branches diverging under the sea floor. This path through the water is the critical path described in the Section 5.3. The diverging paths are influenced by the

velocity of the sedimentary layers through which it travels. Notice that the waves gradually curve through a particular layer and then follow a more vertical path to the surface and a waiting detector. This curvature, which is almost circular, suggests a linearly increasing velocity gradients in these sedimentary layers (cf. Sheriff and Geldart, pages 98-100). Notice that the detectors farthest from the source receive their (first) energy via the deepest refractors. This is because the deepest layers (in this case) have the fastest velocities. This is generally the case although layers with slower velocities are possible. However, lower-velocity layers will not carry the energy to the detector fastest. Of course, energy through the water and any lower velocity layer will get to the detector eventually, just not first. Sheriff and Geldart (page 95 on) describe the critical distance at which refracted energy will appear first. Notice that the lowest (and longest) diving waves are almost parallel to the interface. This suggests a minimal velocity gradient. If there is no velocity gradient, the refracted wave hugs the interface, travelling just below it. This is a head wave described more fully in Section 5.3. Some deep reflections are also shown. They are of no concern for the thesis of this paper.

The thesis I develop in this paper is that seismic diving waves and head waves, which get to the detector before the arrival through the water, can successfully be modeled and used to position the detector. First we examine why this feature is not available to the high frequency acoustic systems used to position OBC detectors.

Absorption

Absorption is the attenuation of sonic energy by conversion into heat in the medium through which it travels. Absorption is treated by Sheriff and Geldart (pages 59-63 and 177-180) and it's a confusing affair. The basic equation for absorption is the following:

$$A = A_0 e^{-\eta x},$$

where A and A_0 are the amplitudes, x is the distance and η is the absorption coefficient expressed in dB per wavelength. In general, through the earth, the higher the frequency (the shorter the wavelength) the more rapidly sonic energy attenuates. This means that acoustic energy (such as that used in a positioning system) at 60 kHz will attenuate in the earth one thousand times faster than seismic energy at, say, 60 Hz. On the other hand, higher frequencies seem to be favored in liquids such as sea water (Sheriff and Geldart, page 177).

The net consequence of these facts is that acoustic energy travels from the pinging vessel to the transponder (attached to the seismic detector) only through the water, not through the earth. On the other hand, seismic energy travels to the detector both through the water and through the earth. Depending on layer depth, relative velocities and the critical distance mentioned in the Section 5.1 and defined in Section 5.3, the first arrival may be through the earth.

As an important aside, this is good news for the positioning of detectors by seismic energy in very deep water. Velocity gradients exist in the water as well as in the earth. The deeper the water, the more significant the velocity gradient is likely to be, with a consequent impact on acoustic positioning results, as acknowledged by Caldwell. Unfortunately, we don't have acoustic transponders in the water column to measure the velocity gradient; a velocity probe must be used, thus requiring additional expense and operational inconvenience. But we do have seismic detectors along the ocean bottom to measure the velocity gradient in the refractor without deploying additional sensors. Seismic time in the water column is a static delay that can be solved and removed. A method of doing so is discussed in Section 7.1.

Head Waves versus Water Waves

Issues of refracted head waves, water waves and the critical angle are illustrated in Figure 4. The source is just under the water at the asterisk (*). The detector is to the right on the bottom (O). The water depth under the source is zs. The depth of the detector relative to the source is zd. The water velocity is v0. The velocity of the ocean bottom is v1, which is greater than v0. A method for determining v1 is given in Section 7.1. We usually observe water velocity near the surface on an OBC crew, especially one using acoustics. The bottom slopes gently.

The critical angle mentioned above is i. Following Sheriff and Geldart (page 63), it is defined as

$$i = \arcsin(\frac{v0}{v1})$$

Since zs is an observed quantity, we can now compute the distance through the water into the refractor (S) and the other side of the triangle along the bottom (C).

$$S = \frac{zs}{\cos(i)}$$

$$C = zs \cdot \tan(i)$$

In this case, where the detector is at the bottom of the first layer, the critical distance less than which refracted energy will not be seen is C. If the detector were at the surface, the critical distance would be 2C.

Let TT be the travel time of the first break pick, our observation in the positioning algorithm we are developing. First breaks are discussed in Section 6. If TT is greater than S/v0, the length of time in the water column into the water-bottom refractor, then we know that TT is a refracted arrival. Otherwise, it's a water arrival, which implies that the detector's horizontal distance from the source is less than C.

TT minus S/v0 is the time in the refractor. Multiplying that quantity by the refractor velocity v1 gives us the distance in the refractor (R). Expressed mathematically:

$$TT = \frac{S}{v0} + \frac{R}{v1}$$

$$R = (TT - \frac{S}{v0}) \cdot v1$$

Now, the direct seismic water arrival travels down the path (D). The gentle slope notwithstanding, we can approximate the later water arrival as follows, first as the distance D(dist) and then as the time D(time).

$$D(dist) = \sqrt{zd^2 + (C + R)^2}$$

$$D(time) = \frac{\sqrt{zd^2 + (C + R)^2}}{v0}$$

The water arrival at D(time) is buried in the seismic record.

In the case of acoustics, D(time) is all the transponder "sees" due to high-frequency acoustic attenuation in the earth. If the water depth is shallow there will be guided acoustic reverberations between the surface and the bottom like a channel wave (Sheriff and Geldart, page 483).

Consequently, acoustic pinging is done at close range in shallow water. Although range is not a limitation for refracted seismic arrivals, range and depth are limitations for acoustic systems. One vendor is limited to 500 meters range through the water. Another vendor is limited to 500 meters of transponder depth (due to pressure considerations).

Ray Tracing a Geological Model That Produces Head-Wave Pick Times

The validity of a positioning algorithm can be checked in three ways: (1) comparison with a secondary system, (2) comparison of split data sets (either randomly or into nears and fars) and (3) processing simulated (synthetic) data sets. This section deals with one aspect of method (3), ray tracing a geological that produces simulated head wave pick times.

The geological model is given in Figure 5. It consists of a water layer 200 meters thick with a velocity of 1500 m/s, a first refracting layer 100 meters thick with a velocity of 2000 m/s, a second refracting layer 100 meters thick with a velocity of 3000 m/s, and a half space with a velocity of 5000 m/s. All layers are flat and homogeneous with constant velocities within the layers. This a simple case, but it does produce a water arrival and three refracted head-wave arrivals depending on the critical distances. There are no diving waves. The simulated results will provide an excellent workout for the positioning algorithm described in Section 7.

The ray tracing code in Matlab that follows is well annotated. It exhibits the principles of ray tracing refracted energy described by Sheriff and Geldart (pages 95-98). First coordinate configuration files for the detectors and the sources are read. Then the geological model is defined. Next, some important angles are defined. For example, for the third (deepest) refractor, i34 is the ray parameter and the incident angle into the half space, i24 is the incident angle is the layer above and i14 is the incident angle in the water. The critical angle into the first refractor is i12. And so on. Next, the critical distances of the three refractors are computed. Later in the code all arrivals that are beyond the critical distances are computed, some random noise is added and the minimum of the four possible arrivals is selected. Then the pick is rounded to 2ms to emulate the sample interval. Also a 100ms static offset is added to emulate instrumental or picking delay. The processing algorithm will solve for this delay (see Section 7.1). The Matlab code follows:

```
% simnew5.m  4/3/99   Simulate FB picks from a geological model.


% Set-up procedures:
% ******************

% Set random number seed to some number
randn('seed', 5348);

% Read configuration file for detectors
% Define the coordinates of the detectors
load simdet5.dat
detect = simdet5;
[dstations, n] = size(detect);
fprintf('dstations are %6.2f \n', dstations);

% Read configuration file for sources
% Define the coordinates of the sources
load simgps5.dat
source = simgps5;
[sstations, n] = size(source);
```

```matlab
fprintf('sstations are %6.2f \n', sstations);

% Define the geological model of the subsurface
% There are 4 possible paths to a detector:
% water, 1st, 2nd and 3rd refractors
paths = 4;
% Water depth is 200m and velocity is 1.5 m/ms
h1 = 200;
v1 = 1.500;
% 1st refractor is 100m thick and 2.0 m/ms
h2 = 100;
v2 = 2.000;
% 2nd refractor is 100m thick and 3.0 m/ms
h3 = 100;
v3 = 3.000;
% 3rd refractor is a half space at 5.0 m/ms
v4 = 5.000;

% Compute some important angles:
% These trace the ray parameters for all 3 refractors
% 3rd refractor
i14 = asin(v1/v4);
i24 = asin(v2/v4);
i34 = asin(v3/v4);
% 2nd refractor
i13 = asin(v1/v3);
i23 = asin(v2/v3);
% 1st refractor
i12 = asin(v1/v2);

% Compute all 3 critical distances.
Xcrit12 = h1*tan(i12);
Xcrit23 = h1*tan(i13)+2*h2*tan(i23);
Xcrit34 = h1*tan(i14)+2*(h2*tan(i24)+h3*tan(i34));

% Setup the observation file
numobs=sstations;
observe = zeros(numobs*12, 5);

% Initialize the observation counter
obs = 0;

% Cycle through all the sources
for thissource = 1:sstations
   thissource

   % Cycle through all the detectors in the array
   for thisgroup = 1:12
      % thisgroup
      picks=zeros(12,1);

      for ii = 1:12
         thisdetect = (thisgroup-1)*12+ii;

         % Compute the source-detector distance with
         % Inverse5 subroutine
         [thisdist, trend] = inverse5(thissource, thisdetect, ...
```

```matlab
          source2, detect2);
      trend = 1;

      % Initialize all 4 breaks to large numbers
      breaks=10000*ones(4,1);

      % Compute the direct arrival.
      breaks(1) = sqrt(thisdist^2+h1^2)/v1;

      % Compute the refracted arrival in the v1/v2 boundary.
      if thisdist > Xcrit12
         breaks(2) = h1/cos(i12)/v1 + (thisdist-Xcrit12)/v2;
      end

      % Compute the refracted arrival in the v2/v3 boundary.
      if thisdist > Xcrit23
         breaks(3) = h1/cos(i13)/v1 + 2*h2/cos(i23)/v2 + ...
            (thisdist-Xcrit23)/v3;
      end

      % Compute the refracted arrival in the v3/v4 boundary.
      if thisdist > Xcrit34
         breaks(4) = h1/cos(i14)/v1 + 2*h2/cos(i24)/v2 + ...
            2*h3/cos(i34)/v3 + (thisdist-Xcrit34)/v4;
      end

      % Choose the minimum pick with 10ms random noise.
      picks(ii) = min(breaks+10*randn(4,1));
   end

   % Emulate a 2ms sample interval
   pick = 2*round(min(picks)/2);

   % Emulate static 100ms instrument and/or picking delay
   pick = pick + 100;

   % Record the pick if less than 2.5 seconds
   if (pick < 2500)
      obs = obs + 1;
      observe(obs, 1) = 10;
      observe(obs, 2) = source2(thissource, 1);
      observe(obs, 3) = detect2(thisdetect, 1);
      observe(obs, 4) = pick;
      observe(obs, 5) = thisdist;
   end
   end
end
end

% Strip out the blank observations
[i,j] = find(observe(:,1)==10);
observe = observe(i,:);
```

First Break Picking

The many paths seismic energy may travel between the source and the detector are described in the previous section, which regards these paths as rays. However, when the energy arrives at the

detector, its form is that of a trace, a long, complicated wave that is the convolution of the source signature with the impulse response of the earth. Our job is to map that trace into a single time event that represents the onset of energy, a first-break pick.

Figures 6, 7 and 8 show 200ms samples of 3 of 5 raw traces (no pre-processing) from the Teal South survey chosen to exhibit the onset of energy. All five traces were recorded by the same hydrophone. They were generated by five different source events (same source) on five different shot lines. They were chosen to sample the range of offsets used in the positioning algorithm: 634, 544, 442, 338 and 220ms respectively as picked by the production first-break picker. The sample interval is 2ms. Notice that the shorter the offset, the more clearly defined is the onset of energy. These traces are analyzed using Matlab in the following three subsections, which explore different ways of making a first-break pick. Section 6.4 discusses different ways to evaluate the quality of a first-break pick, the counterpart of Section 3.2, which discusses the quality of an acoustic range.

Generic Picking Algorithm

An algorithm for an automated first-break picker might go something like this: (1) get the maximum amplitude in the trace, (2) define a test value by dividing the maximum amplitude by some factor, (3) move down the trace 1 sample at a time in a group of 5 samples, (4) compute the average amplitude of the 5 traces, (5) compare the average with the test value and (6) if the test value is exceeded, then back up one sample. We've got our pick.

Implemented in Matlab code, it looks like the following:

```
% genpick1.m  4/4/99   Generic first-break picker

clear pick;  % Results from previous run of the code

% Get the dimensions of the array holding the trace samples
% Note that the first 2 rows are source and detector IDs
[samples, numt] = size(nt1);

% Set the ratio of max amplitude to sample average amplitude
SRS = 25;

% Cycle through the number of traces (numt)
for trace = 1:numt

   % Get the maximum amplitude for this trace
   most = max(abs(nt1(3:samples,trace)));

   % Start at the 5th sample (5+2=7) and move to end
   for samp = 7:samples

      % Compute the mean of these 5 samples
      thismean = mean(abs(nt1(samp-4:samp,trace)));

      % Test if over the threshold
      if thismean > most/SRS
         % Record the pick time one sample retarded
         % Note 2 ID records plus 1 retard (2+1)*2=6
         pick(trace) = samp*2-6
         break
      end
   end
```

```
end
```

Running this code on the 5 traces from Teal South produces the following results:

    pick = 634 542 442 338 220

These values compare well with the production picks. Four are the same; one differs by a sample (2ms).

Cross Correlation

Anstey (1964) describes correlation as " a good method of measuring the similarity between two waveforms (by multiplying) them together, ordinate by ordinate, and (adding) the products over the duration of the waveforms". Measuring different traces is cross correlation; measuring the same trace for repeatability is auto correlation. Sheriff and Geldart describe the use of cross correlation for determining time shifts between traces as, for example, an aid in statics determination (pages 285-290). The basic equation is:

$$\Phi_{xy}(\tau) = \sum_k x_k \, y_{k+\tau},$$

where *x* and *y* are the two (discrete, digital) data sets. A continuous version of cross correlation also exists. An equation for normalized cross correlation (in which correlation values vary between –1 and 1) is given by Sheriff and Geldart (Eq. 9.54).

There could be problems with our generic picking algorithm in Section 6.1 on some difficult data sets. By illustration, at any stage of the algorithm only 6 samples are involved, the one maximum amplitude in the trace and the 5 rolling samples. These few samples may not be adequate to determine the exact onset of energy in some cases. In these cases, better results might be achieved if more samples were used in the identification. Cross correlation accomplishes this. Of course, the product of cross correlation is a first-break pick *difference* involving two traces, not a discrete pick for one trace, but many creative ways to utilize this product can be envisioned.

Figures 9, 10 and 11 plot the normalized cross correlations produced in Matlab between traces 1 and 3, 1 and 5, and 3 and 5 respectively. The X axis is the lag in milliseconds. In theory, there should be a distinct peak, a positive correlation value, the closer to 1 the better, that will define the time lag between the two traces. (A negative correlation value indicates an inversion of one of the traces.) In practice, the interpretation of these correlation plots is more ambiguous than the theory!

The Matlab printout below (lagmat) gives the results from the batch processing of all combinations of cross correlations among the 5 traces. The largest positive cross correlation value is identified and its lag printed in the matrix. It is followed by another printout (pckmat) that gives the same differences derived from the generic picking algorithm in Section 6.1. By way of explanation, there are 5 rows and 5 columns. The number in the 3rd row and 4th column is the difference between traces 3 and 4.

```
lagmat =

      0     96    192    332    470
    -96      0     98    256    374
   -192    -98      0    100    226
   -332   -256   -100      0    118
   -470   -374   -226   -118      0
```

```
pckmat =

      0     92    192    296    414
    -92      0    100    204    322
   -192   -100      0    104    222
   -296   -204   -104      0    118
   -414   -322   -222   -118      0
```

Notice the differences between our generic first-break picker (pckmat) and cross correlation (lagmat)! Which values are preferable? Which are correct? Do the different travel geological paths of the traces at different offset and azimuths vitiate the cross correlation? Is our generic picker really better? Or is cross correlation? Answering these questions (perhaps in Dr. Zhou's Processing class next Fall) is a continuing academic and professional interest for the author of this term paper.

Band-Pass Filtering

Band-pass filtering is a method often employed in production processing to improve the quality of first-break picking. To test the efficacy of band-pass filtering I chose a simple, 5-point, zero-phase 60 Hz high-cut Butterworth filter. (The "zero-phase" feature of this filter in Matlab mean that it is applied beginning to end and end to beginning. A normally applied filter (beginning to end) seems to shift the trace in time.) I applied the filter to the 5 Teal-South traces. Figure 12 shows the results of the filter on Trace 3. Compare Figure 12 with Figure 7, the raw trace.

Then I ran our generic picker (Section 6.1) on the 5 filtered traces. The Matlab printout below gives the results.

```
pick  =  628    536    428    332    204
```

Then I cross correlated (Section 6.2) the 5 filtered traces. The Matlab printout below gives the results.

```
lagmat =

      0     96    228    328    434
    -96      0    102    208    380
   -228   -102      0    102    224
   -328   -208   -102      0    122
   -434   -380   -224   -122      0
```

Again, notice the differences with the use of the generic picker and cross correlation on the raw traces (Sections 6.1 and 6.2)! Which values are preferable? Which are correct? Unfortunately, I present more questions than answers in these sections.

Pick Quality

The difficult of assessing the quality of a first-break pick is clear from the preceding three sections. Even if we accept a specific automated method as authoritative (such as our generic amplitude picker), it is difficult to judge algorithmically when it is likely to fail, to *predict* its quality. Also, it needs to be calibrated against picks made by the hand of a geophysicist. Fortunately, we have another way of assessing the quality of a first-break pick, namely, the positioning algorithm discussed in Section 7. Good picks will "group" well about the computed

coordinates, i.e., their residuals will be small. Poor picks will have large residuals. Absolutely egregious picks will need to be rejected as blunders (outliers). The quality of the coordinates predicted by the positioning algorithm will depend upon the grouping of the first-break picks.

So, unlike the electronic assessment of acoustic resolution (Section 3.2), first breaks pickers don't lend themselves to a native assessment of quality. But the quality of both acoustics and first breaks can be assessed by the residuals in their respective adjustment algorithms. Acoustic residuals are about 0.6 to 1.0m (expressed as a standard deviation). First-break residuals vary. Often they are comparable to the sample interval (2 or 4ms) times the speed of sound (about 3 to 6 meters). Sometimes they can be better, sometimes worse. The results of the positioning algorithm are driven by the quality of the first-break picks. This fact has motivated my study of geophysics.

First Break Positioning Algorithm

Now I briefly describe the main features of a generic first-break processing algorithm capable of resolving the first-break pick times derived from diving waves and refracted head waves as described in Sections 5 and 6. It is like the one used to process the Teal South data reported in this paper. First, a global polynomial regression pre-processor relates pick time to distance in three dimensions and solves for several systematic errors. Blunder rejection is implemented in the global polynomial regression stage with a difference tolerance. Then, regressed distances are adjusted by least squares to determine optimal detector coordinates Revised coordinates mean revised offsets, a different global polynomial and new regressed distances. The algorithm is iterated until convergence. Finally, geodetically-significant quality control measures are reported.

Global Polynomial Regression

Our observations are the seismic first-arrival picks. A pick is associated with nominal coordinates and depths for the source and the detector. The distance (or offset) between these nominal coordinates can be determined using the Pythagorean Theorem in three dimensions. Using least squares, offsets are regressed against pick times to determine the coefficients of the best-fitting polynomial of a user-selected order. Using this polynomial, a "regressed" distance in meters or feet is determined for a specific pick in milliseconds by substitution into the polynomial. These regressed distances are processed by least-squares estimation.

Figure 13 shows computed distances in meters plotted against pick times in milliseconds for the Teal South data set, more than 100,000 first-break picks. Sight along this plot at an angle to see the vertical velocity gradient. A polynomial fitted to these points determines the relationship between pick times and regressed distances that are processed by the measurement model. Notice that the polynomial does not cross the origin of the plot. This static, Y-axis intercept at zero pick time absorbs the systematic errors of instrumental delay and delay (or anticipation) in the mathematical definition of the onset of seismic energy in the first-break picker. The shape of the polynomial at near offsets will correct for a global bias in bathymetry by bending into an approximate hyperbola. Outlying picks are shown on this plot. They are rejected if they exceed a difference tolerance with respect to the polynomial. This improves coordinate results and predicted coordinate error.

The form of the normal polynomial is as follows:

$$ptd = c_0 + c_1 \cdot pt + c_2 \cdot pt^2 + \cdots + c_n \cdot pt^n,$$

where *ptd* is pick time (or regressed) distance, *pt* is first-break pick time, c_0 through c_n are the coefficients of the best-fitting polynomial estimated by least squares, and *n* is the order of the polynomial, which is user selectable. Differentiating the polynomial with respect to pick time provides an equation of the slope of the global polynomial. This can be interpreted as velocity (Δdistance/Δtime) over the refracted travel path as a function of pick time. The form of the differentiated polynomial is as follows:

$$sv = c_1 + 2 \cdot c_2 \cdot pt + 3 \cdot c_3 \cdot pt^2 + \cdots + n \cdot c_n \cdot pt^{n-1},$$

where *sv* is the slope (a velocity).

If a first-order polynomial is chosen and the residual offsets plotted as a function of pick time, the character of the different refractors (there may be several) can be seen as distinct velocity transitions or as continuous transitions (diving waves).

Many of the features of the global polynomial regressing discussed above are covered by patent (Zinn and Chambers, 1997). Other methods of accomplishing the same objectives can easily be envisioned.

Least-Squares Estimation

The equations of a least-squares positioning algorithm are widely published in the literature (Cross 1983, Sheriff and Geldart pages 293-295). Ignoring the vertical component for simplicity, our basic observation equation is:

$$ptd = \sqrt{(X_S - X_D)^2 + (Y_S - Y_D)^2},$$

where (X_S, Y_S) and (X_D, Y_D) are source and detector coordinates respectively and *ptd* is the pick time (or regressed) distance above. Using the first-order terms of a Taylor's Series expansion of *ptd*, the linearized observation equation is:

$$\Delta ptd = \frac{\partial(ptd)}{\partial(X_D)} \cdot \Delta X_D + \frac{\partial(ptd)}{\partial(Y_D)} \cdot \Delta Y_D,$$

which, with a little calculus, reduces to

$$\Delta ptd = -\frac{(X_S - X_D)}{ptd} \cdot \Delta X_D - \frac{(Y_S - Y_D)}{ptd} \cdot \Delta Y_D$$

which, with a little trigonometry, further reduces to

$$\Delta ptd = -\sin(\alpha) \cdot \Delta X_D - \cos(\alpha) \cdot \Delta Y_D,$$

where α is pick azimuth.

Since I wish to balance geodesy with geophysics in this term paper, further least-squares equations are not reproduced here. Our algorithm will adhere to the conventional approach of forming and inverting the matrix of coefficients of the normal equations, which consist of the $\sin(\alpha)$ and $\cos(\alpha)$ terms derived above, to solve for coordinates (cf. Sheriff and Geldart, op. cit.).

Iteration Until Convergence

The basic observation cited above is non-linear (linearized by Taylor series expansion). Consequently, both stages of our first-break positioning algorithm must be iterated in sequence

until coordinate convergence to some user-defined tolerance. If our modeling is good, convergence will be rapid.

Quality Control

Our algorithm should and does provides a wealth of geodetic quality control statistics by which to evaluate results. These include the unit variance factors for all detectors (which quantify the "fit" of the adjustment given pick uncertainty), coordinate variances and covariances in the grid axes (from which the "error ellipse" can be derived), dRMS (distance root mean square, or radial error) values scaled by the unit variance factor that predicts coordinate quality, the number of rejected picks, the total number of used picks for each detector and the number in each octant and the coefficients of the best-fitting polynomial. Also, plots of residuals as a function of pick time and the usual seismic quality control of linear moveout (LMO) corrected first arrival displays can be produced to examine visually the affect of the recomputed coordinates on the seismic alignments.

Comparisons of Coordinate Results in Teal South

Error Quantification and Compensation

Like all measurement systems, both acoustics and first breaks have sources of random, systematic and gross error that must be quantified, modeled or eliminated by the positioning software. Both are affected by the geometrical distribution of observations. It is important that observations are collected from all quadrants around the detectors or transponders. Unbalanced geometry decreases the reliability of the solution if gross observational errors (blunders, spikes, outliers) occur (as they will) and are undetected. Unbalanced geometry also decreases the ability of a first-break positioning algorithm to solve for systematic errors in the global regression stage.

Acoustics and first breaks share some sources of systematic error (deterioration of GPS positioning, instrumental delays, uncertainties in depth and the velocity of propagation in water), but differ in others. Acoustics are more affected by surface ghosts and bottom obstructions. First breaks are more affected by lateral variations in refractor velocity (layer inhomogeneity) and complex geology. Their respective adjustment software must model and solve for these sources of systematic error. Gross errors must be identified and eliminated by both systems. A comparison of acoustic and first-break coordinates is a test of how well all this has been accomplished.

Summary of Comparisons

Figure 14 is a bullet plot of the comparison of 24 coordinate pairs from the survey. All but one difference is less than 2 meters. The mean differences are sub-meter in both the X and Y coordinates and the random scatters about the mean in X and Y are also sub-meter in standard deviations. This agreement confirms that both systems are free from major systematic biases, although a small bias (in one system or another, or both) and the expected random differences do remain. It is reassuring that these disparate but complementary technologies agree to within seismically-acceptable tolerances.

Conclusion

This paper has described a method of using seismic energy that has refracted through the sub-surface to position seismic detectors placed on the ocean bottom, a synergism of geophysics and

geodesy. I have drawn extensively on material from our Seismic Wave and Ray Theory class to support my reasoning. First-break positions are considerably cheaper than acoustic positions to acquire. Properly executed, first-break and acoustic positions compare well. Used together, both seismic first breaks and acoustics provide positioning redundancy.

Acknowledgements

Any creative effort is advertently or inadvertently influenced by the work of others. Below I list some of the advertent borrowings in this paper.

Figures 1 and 3 were created by my company's graphics department.

Figure 14 was plotted in Excel by a co-author, Jay Bole. See references.

Some parts of the OBC overview in Section 2, specifically, the several advantages of OBC over marine streamers, were described to me by a colleague.

Much of the description of the Teal South 4-D/4-C survey in Section 4 is due to another colleague and co-author, Martin Stupel. See references.

The relationship between the refracted and direct travel paths in Section 5.3 was described to me by yet another colleague.

I have, of course, extensively consulted our text, *Exploration Seismology*, which is cited extensively in the paper.

The acknowledged material above is generally background or illustrative and not germane to the demonstration of my thesis, namely, that seismic energy is a viable positioning method for OBC. Otherwise, the rest of the paper and the integration of the advertent borrowings is my own original work.

References

Anstey, N.A., *Correlation techniques - A review*, Geophysical Prospecting, 1964, 12: 355-82

Bole, J., Zinn, N., and Stupel, M., *Seismic Detector Positioning in a 4-D/4-C OBC Survey Using both Acoustics and First Breaks*, EAGE, 1988

Cross, P.A., *Advanced least squares applied to position fixing*, University of East London, Department of Surveying, Working Paper Number 6, 1983

Ebrom, D., Krail, P., Ridyard, D., Scott, L., *4-C/4-D at Teal South*, The Leading Edge, October 1998

Gelb, A., 1974, *Applied Optimal Estimation*, MIT Press

Partridge, S. and Zinn, N., *Positioning Ocean Bottom Seismic Cables*, OTC, 1999

Ridyard, et al, The Leading Edge, 1998

Sheriff, R.E. and Geldart, L.P., *Exploration Seismology*, Cambridge University Press, 1995

Zinn, N., *Modeling Velocity Gradients in an OBC, First-Break Positioning Algorithm*, EAGE, 1997

Zinn, N., *Ocean-Bottom Cable Detector Positioning: Acoustics versus First Breaks*, The Hydrographic Journal, No. 87, January 1998

Zinn, N. and Chambers, R., *Method for Verifying the Location of an Array of Sensors*, U.S. Patent Number 5,696,733, December 9, 1997.

Zinn, N. and Rapatz, P.J.V., *Positioning Networks in 3D Marine Seismic*, OTC, 1993

Graphics follow on next pages

Figure 1: The Elements of an OBC Survey
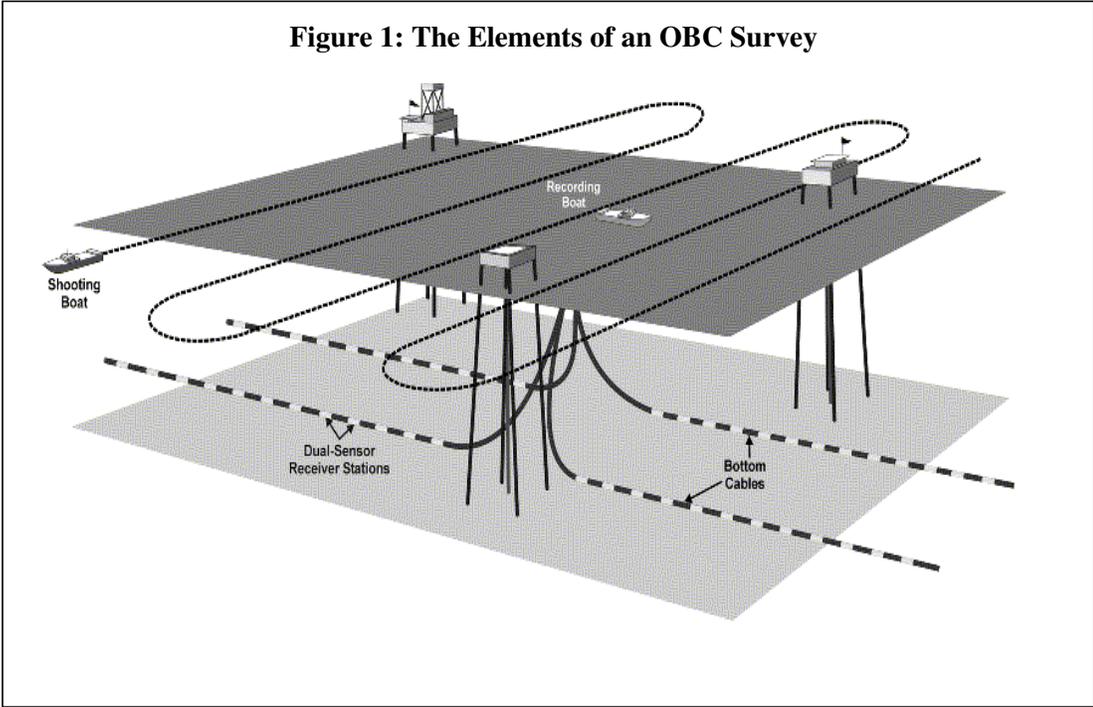
Figure 2: Teal South Prospect

-182,600

Northings in Feet

-191,000

1,868,000   Eastings in feet   1,877,000

Figure 3: The Many Paths of Seismic Energy

Figure 4: Geometry of Refracted Arrival
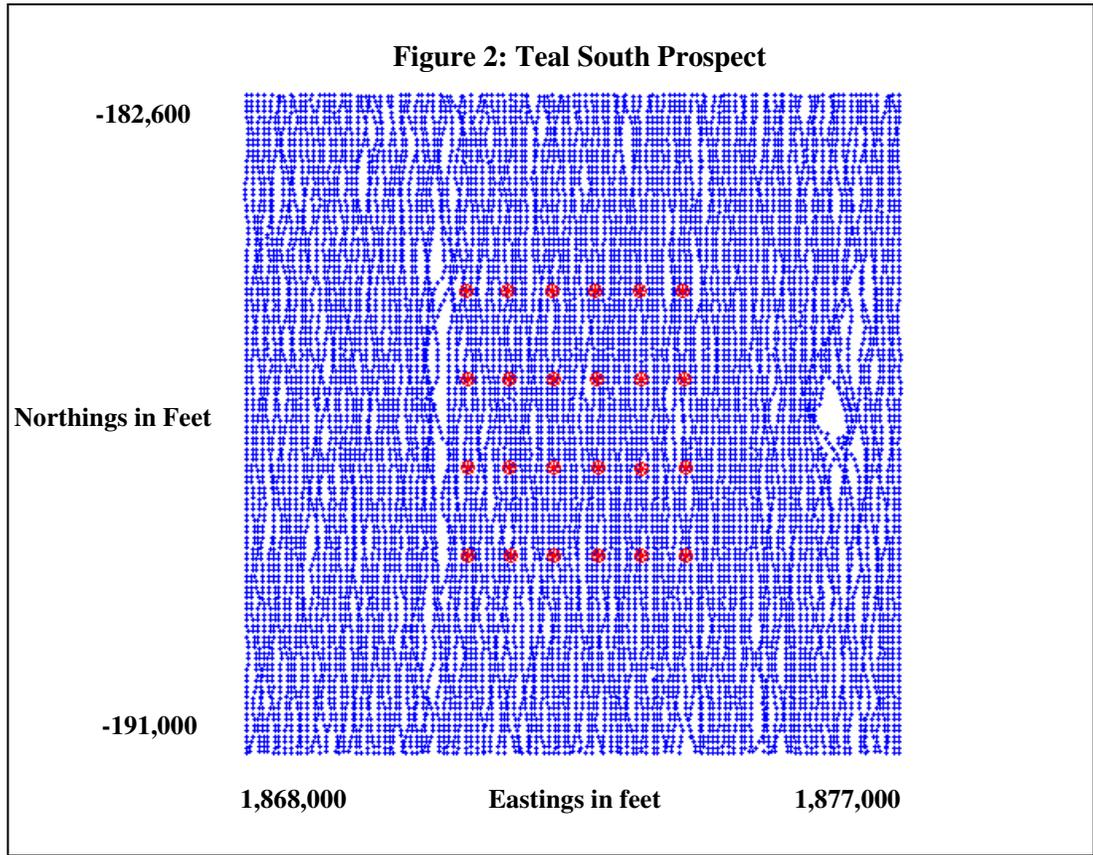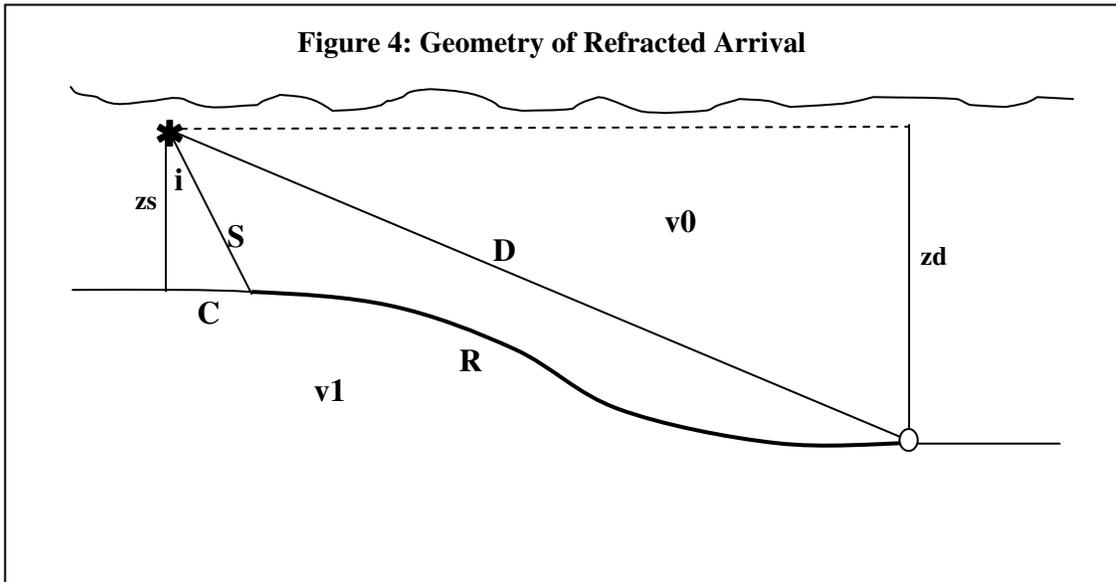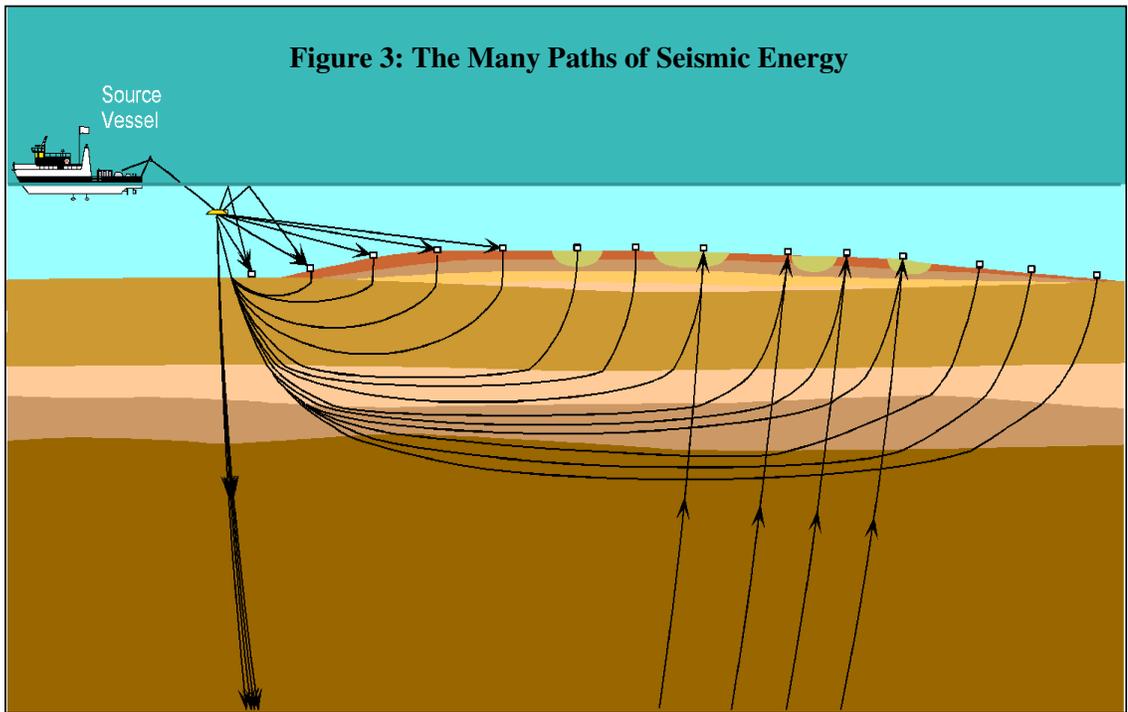
Figure 5: Geological Model in Depth

h = 200m   v = 1500m/s

h = 100m   v = 2000m/s

h = 100m   v = 3000m/s

half space   v = 5000m/s
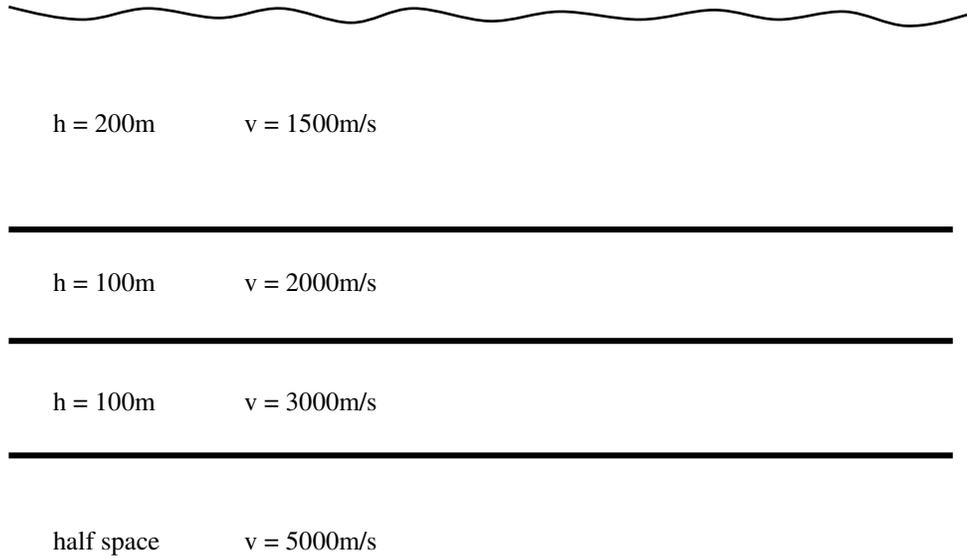
Figure 6: Trace 1
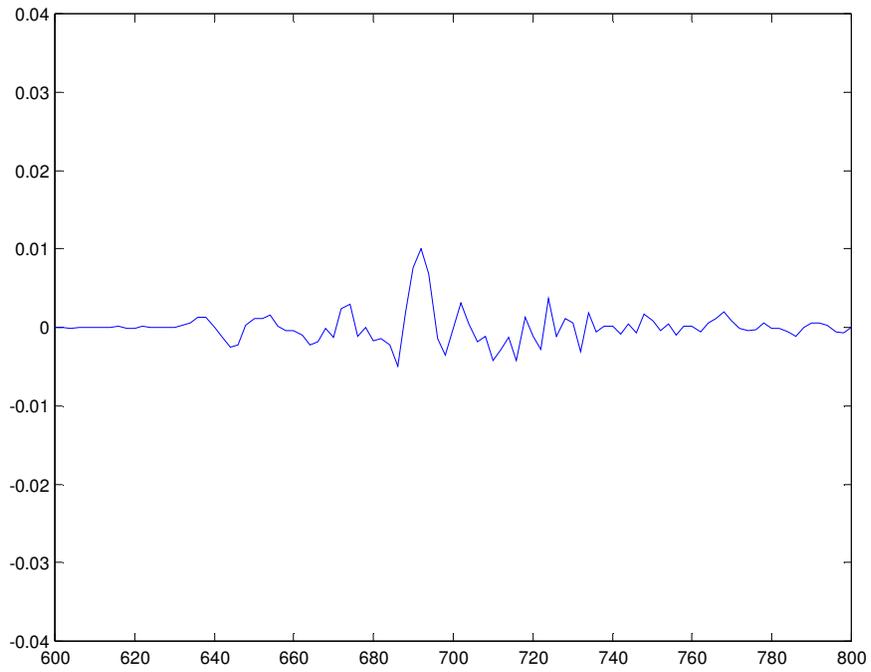
Figure 7: Trace 3
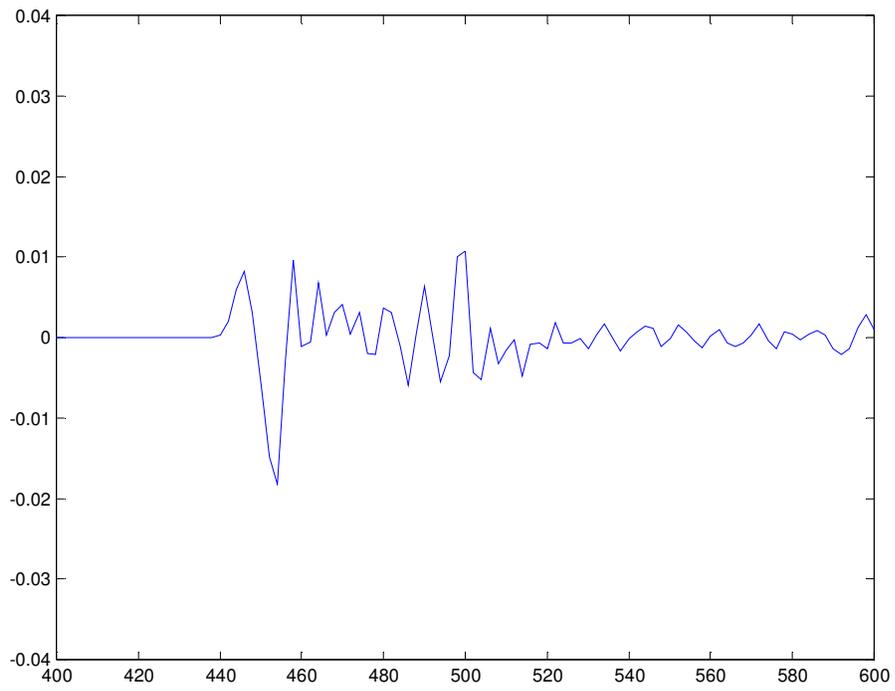
Figure 8: Trace 5
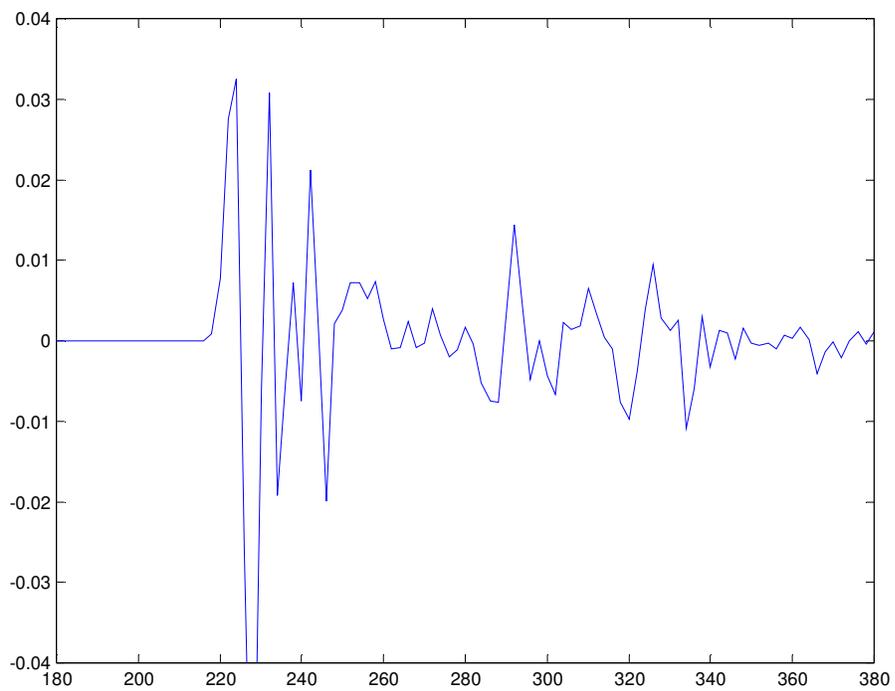
Figure 9: Cross Correlation Traces 1 and 3
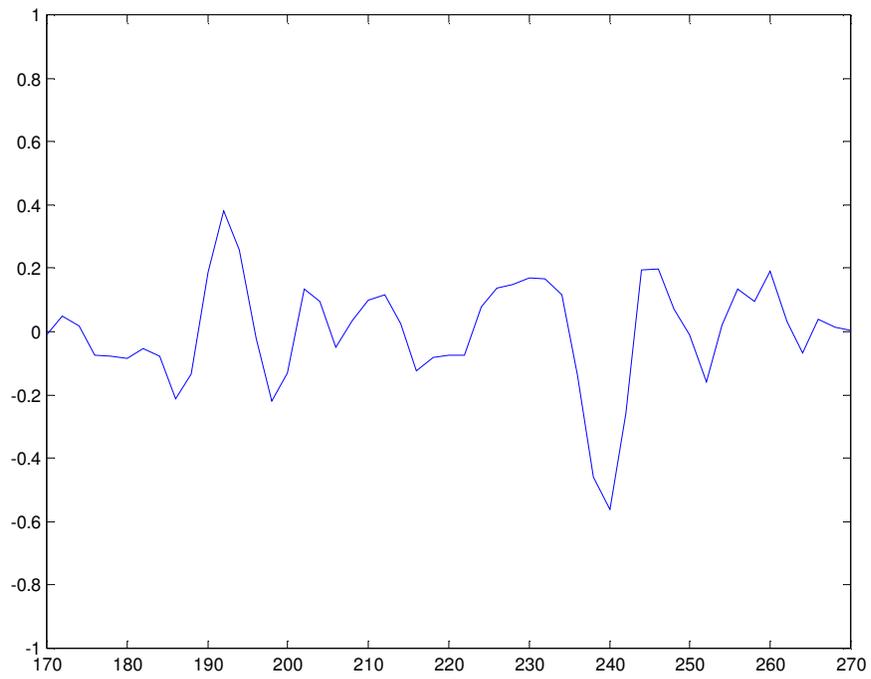
Figure 10: Cross Correlation Traces 1 and 5
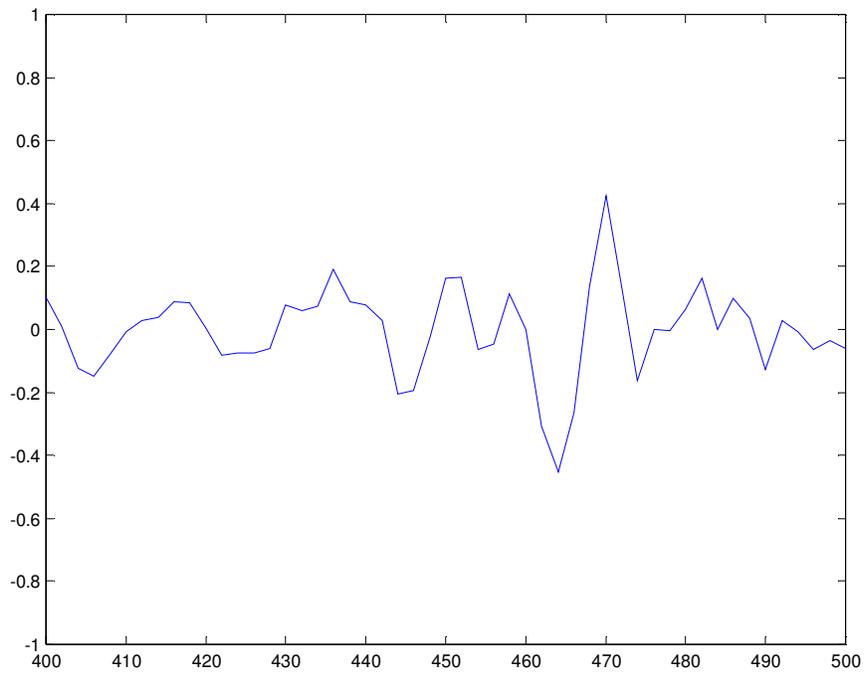
Figure 11: Cross Correlation Traces 3 and 5
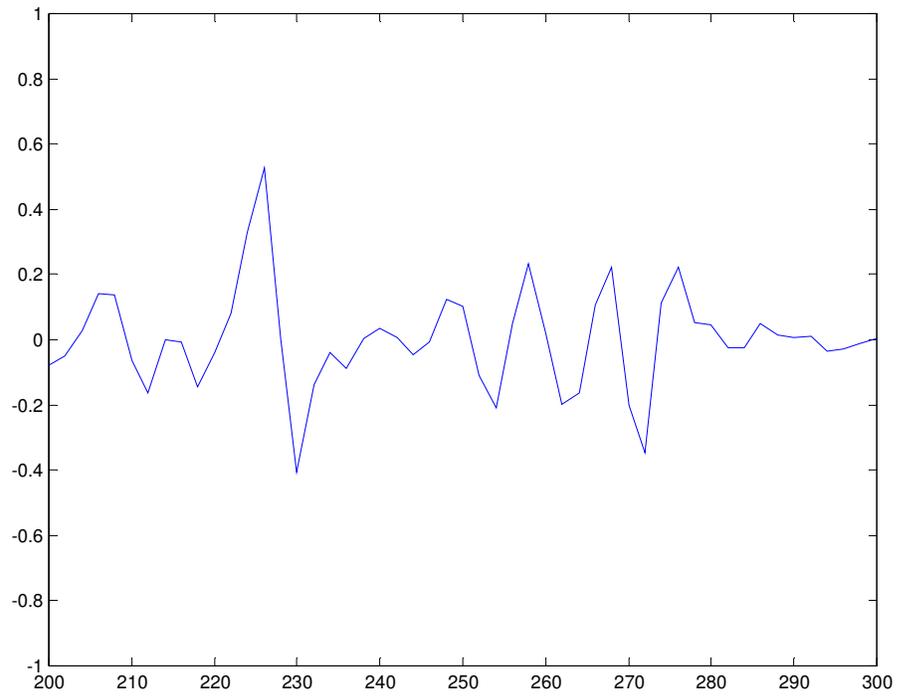
Figure 12: Trace 3 with 60Hz High-cut Filter
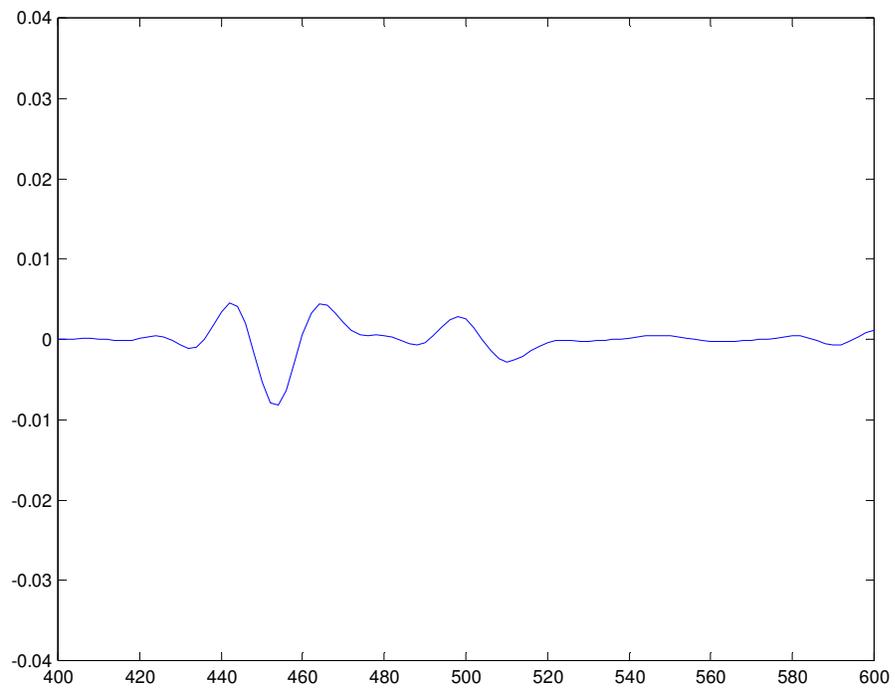
Figure 13: Offset versus Pick Time
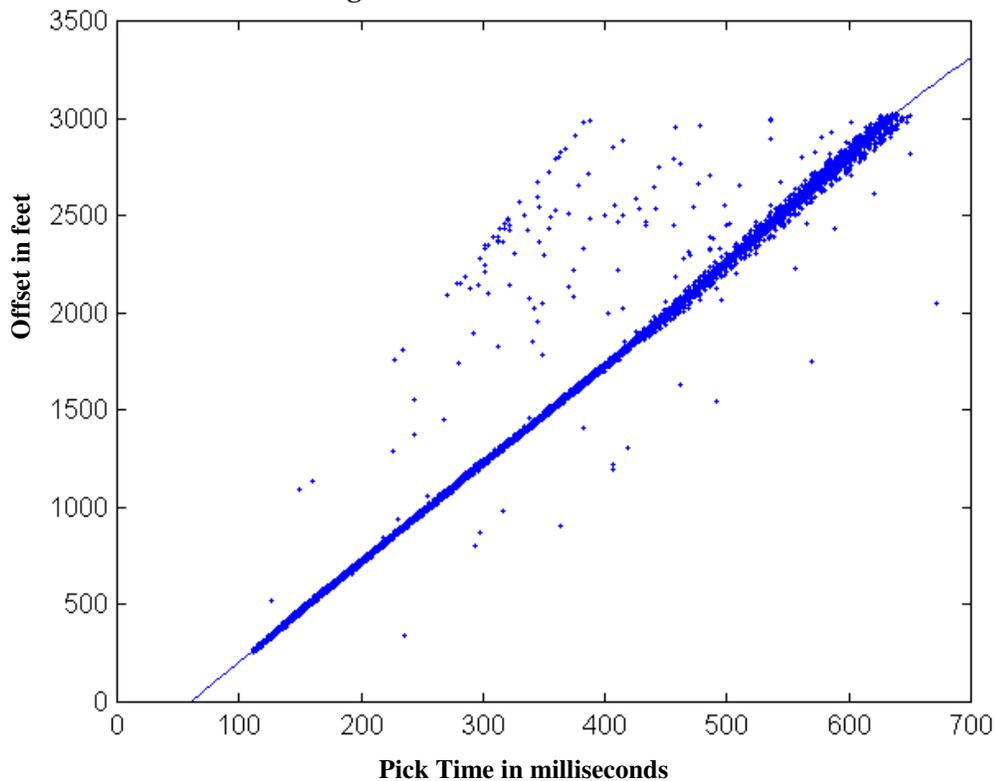
Figure 14: Teal South Acoustic versus First-Break Differences